34th Annual International Conference of the IEEE EMBS
San Diego, California USA, 28 August - 1 September, 2012

High Performance 3-coil Wireless Power Transfer System for the 512-electrode Epiretinal Prosthesis

Yu Zhao, Mandheerej Nandra, Chia-Chen Yu, Yu-chong Tai

***Abstract* — The next-generation retinal prostheses feature high image resolution and chronic implantation. These features demand the delivery of power as high as 100 mW to be wireless and efficient. A common solution is the 2-coil inductive power link, used by current retinal prostheses. This power link tends to include a larger-size extraocular receiver coil coupled to the external transmitter coil, and the receiver coil is connected to the intraocular electrodes through a trans-sclera trans-choroid cable. In the long-term implantation of the device, the cable may cause hypotony (low intraocular pressure) and infection. However, when a 2-coil system is constructed from a small-size intraocular receiver coil, the efficiency drops drastically which may induce over heat dissipation and electromagnetic field exposure. Our previous 2-coil system achieved only 7% power transfer. This paper presents a fully intraocular and highly efficient wireless power transfer system, by introducing another inductive coupling link to bypass the trans-sclera trans-choroid cable. With the specific equivalent load of our customized 512-electrode stimulator, the current 3-coil inductive link was measured to have the overall power transfer efficiency around 36%, with 1-inch separation in saline. The high efficiency will favorably reduce the heat dissipation and electromagnetic field exposure to surrounding human tissues. The effect of the eyeball rotation on the power transfer efficiency was investigated as well. The efficiency can still maintain 14.7% with left and right deflection of 30 degree during normal use. The surgical procedure for the coils' implantation into the porcine eye was also demonstrated.**

I. INTRODUCTION

Age-related macular degeneration (AMD) and retinitis pigmentosa (RP) are two of the most common outer-retina degenerative diseases. Retinal prostheses, which bypass the defective outer-retina photoreceptors and electrically stimulate the inner-retina neurons directly, have achieved light perception in blind people with AMD and RP. Currently most established prostheses only involve a very small number of stimulating electrodes on the neurons. However, to realize facial recognition or large-sized letter reading, the next-generation retinal prosthetic devices demand 1024 stimulating electrodes. Unfortunately, the high-resolution sensors and processors have high power consumption (> 100 mW). In order to minimize the heat dissipation and electromagnetic field exposure, the power transfer efficiency should be optimized in general [1-2].

Although the 2-coil inductive coupling link has been thoroughly studied for wirelessly powering the retinal prosthetic devices, the physical placement of the implanted receiver coil remains a matter of ongoing debate. There are tradeoffs between the power-transfer capability, surgical risk and long-term implantation. The optimal solution is yet to be concluded [3-5]. Generally, the 2-coil inductive link efficiency is proportional to the square of the coupling coefficient (k) and the respective quality factors (Qs) of the coupled coils. To compensate for the low-efficiency of this air-cored coupling and satisfy all safety limitations (the heat dissipation, electromagnetic field exposure, etc.), the receiver coils are placed extraocularly and connected to the electrodes sitting intraocular through a cable that penetrates the eyeball. This trans-sclera trans-choroid cable potentially causes infection and hypotony in the long-term implantation [6]. On the other hand, an ideal fully intraocular retinal implant places the receiver coil inside the lens capsule after removing the natural lens. With a 1-inch separation between the transmitter and receiver coils, our previously optimized 2-coil configuration suffers low efficiency (7 % at the best) from the limited Q of the receiver coil and the small k between the coupled coils.

Herein, we implemented the 3-coil inductive configuration shown in Fig. 1, by adopting the most practical placements of the buffer coil and the receiver coil and using an established surgical procedure of implantation. It's part of a collaborated endeavor to develop a 512-electrode retinal prosthesis.

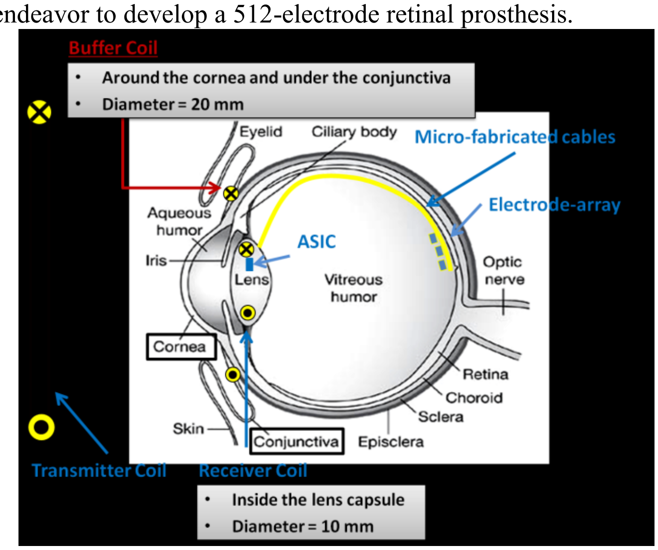

Figure 1. The 3-coil system placement: The buffer coil is implanted around the cornea and under the conjunctiva. The receiver coil is sitting inside the lens capsule.

* The funding is provided by the NSF BMES ERC Center under Award Number H31068.

Yu Zhao is with California Institute of Technology, Pasadena, CA, 91125 USA (corresponding author to provide phone: 626-395-3884; fax: (626) 395-8475; e-mail: yzhao@caltech.edu).

Mandheerej Nandra is with California Institute of Technology, Pasadena, CA, 91125 USA (e-mail: nandra@mems.caltech).

Chia-Chen Yu is with California Institute of Technology, Pasadena, CA, 91125 USA (e-mail: ccyu@caltech.edu).

Yu-chong Tai is with California Institute of Technology, Pasadena, CA, 91125 USA (e-mail: yctai@mems.caltech).

In the 3-coil power system, the transmitter coil was first inductively coupled to the buffer coil placed around the cornea and under the conjunctiva. Instead of using a cable penetrating through the eyeball, this design introduced another inductive link between the buffer coil and receiver coil (in the lens capsule). The insertion of the buffer coil not only eliminated the trans-sclera cable and minimized the possibility of infection and hypotony, but also provided high coupling efficiency. The comprehensive circuit analysis of multiple-coil inductive link can be found in the literature [7-8]. The buffer coil can achieve a much higher Q than the intraocular one, since it's not restricted by the extreme dimension and mass constraints of implanted coils. The high Q compensates the low k between the transmitter and buffer coils, which makes a high-efficiency inductive link. Because the buffer coil is placed in close proximity to the receiver coil, high k between the two coils balances the low Q of the receiver coil for efficient power transfer.

The experimental 3-coil system was used to power the equivalent input impedance of the 512-electrode stimulator chip designed by the Caltech Mixed-mode Integrated Circuit and System Laboratory, for a demonstration.

II. 3-Coil Inductive Coupling Design for Retinal Prostheses

The general design methodology and system optimization of the multiple-coil inductive link have been established [6-7] Therefore theoretical optimal power transmission efficiency can be calculated from coupling coefficients between each two adjacent coils, quality factors of multiple coils, operating frequency and load.

Implementation of the 3-coil link is a multi-dimensional design due to size and mass constraints as well as its ability to be easily implanted. Different from the previously established 2-coil design, the 3-coil inductive link is restricted by a different set of constraints, which limit the degree of freedom in optimizing the efficiency. Given the geometrical specifications listed in Table. 1, the dimensions of the buffer coil and intraocular receiver coil have been largely limited. With the fixed separations, the diameter of the transmitter coil was optimized by COMSOL Multiphysics simulations and measurements to maximize the coupling coefficients. Then the mutual coupling coefficients can be derived respectively.

Table 1. The design specifications of 3-coil link
Transmitter coil: L_1; Buffer Coil: L_2; Receiver coil: L_3;

Geometrical Parameter	***Value***
Outer diameter of L_3	*10 mm*
Maximum mass in aqueous of L_3	*10 mg*
Outer diameter of L_2	*20 mm*
Separation between L_2 and L_3	*4 mm*
Separation between L_1 and L_2	*21 mm*
Separation between L_1 and L_3	*21+4 mm*
Optimal diameter of L_1 (3-coil config)	*42 mm*
Coupling coefficient between L_1 and L_2 ,k_{12}	*0.0334*
Coupling coefficient between L_2 and L_3 ,k_{23}	*0.1377*
Coupling coefficient between L_1 and L_3, k_{13}	*0.0127*

A. Microfabricated origami foil coil as the receiver coil

The lens capsule is an ideal position to place the intraocular receiver coil. After the natural lens is removed, the intraocular coil can be implanted into the lens capsule bag.

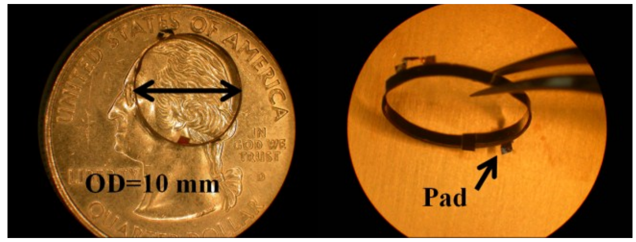

Figure 2. The microfabricated origami foil coil as the receiver coil. The outer diameter is 10 mm.

The implantation surgical procedure is well established [5]. Associated with that implant position, two intrinsic challenges for achieving a high-Q coil are the size (< 10 mm in outer diameter) and mass (< 46 mg in saline), as the lens capsule cannot host a coil that is either too large or too heavy. The MEMS origami foil coil [9] was designed and fabricated to assume the receiver power coil, as shown in Fig. 2. The coil is flexible and foldable, allowing for a minimally invasive implantation. In air, the Q factor was measured to be around 24 at the operating frequency (10 MHz).

B. Hand-wound Litz coil as the buffer coil

The buffer coil with a diameter of 20 mm needs to be implanted around the cornea and under the conjunctiva. The surgical procedure can be found in reference [4]. The coil is hand-wound from commercial 30/48 Litz wire. At 10 MHz, the Q factor can achieve 92 in air.

C. The optimal transmitter coil

The placements and dimensions of both the receiver coil and buffer coil are fixed. With a 1-inch separation, the optimal diameter of the transmitter coil was simulated using COMSOL Multiphysics to maximize the coupling coefficient between transmitter coil and buffer coil. The simulated electromagnetic field distribution around the 3-coil configuration is shown in Fig. 3. The coupling coefficients can be calculated from the field integration. The optimal diameter was found to be 42 mm. The coil was also implemented as a Litz-wire hand-wound coil designed to be mounted on a pair of reading glasses.

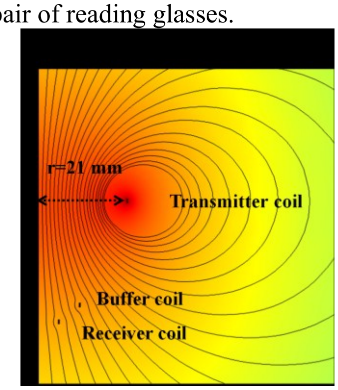

Figure 3. The electromagnetic field distribution in the 3-coil link

D. The electrical specifications

10 MHz carrier frequency was chosen due to a tradeoff between the tissue's RF absorption and coils' Q values. All three coils can be tuned to resonate at the operating frequency with connection to corresponding capacitors in parallel or in series. Table 2 shows the electrical design specifications.

Table 2 The Electrical Specifications

Electrical Parameter	***Value***
Output Voltage across DC load	*1.9 V*
Output power on DC load	*25 mW*
Equivalent AC parallel load R_{dc}	*70 Ω*
Equivalent DC parallel load R_{dc}	*140 Ω*
Q of L_1, Q_1 *and Q of* L_2, Q_2 *(Litz Coil)*	*~100*
Q of L_3, Q_3 *(MEMS Foil Coil)*	*~20*

The receiver coil in parallel with a resonant capacitor will be connected to the customized IC chip, which is expected to receive 25 mW power and a peak-to-peak voltage of 3.7 V. In the proto-type power transfer efficiency measurement setup, the input impedance of the chip was simplified as a diode and capacitive impedance with the equivalent DC resistance of 140 Ω, as show in Fig. 4.

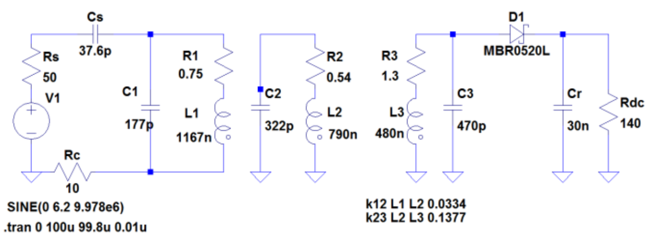

Figure 4. The simulated circuit schematic with LTspice

III. 3-Coil Inductive Link Testing in Saline

A. Device characterization in saline

Both the buffer coil and the receiver coil will be implanted into human tissue, so the Q factors of these coils and corresponding resonating tanks will drop because of the lossy medium (i.e., Aqueous humor). Loss tangent can represent the power loss in the medium. The loss tangent of saline is about 0.2, which is much higher than the air, but close to the body tissue and fluid. This means the electromagnetic energy dissipates more easily in the saline. Therefore, the Q factors of the buffer coil and the receiver coil were characterized in saline. The addition of the low dielectric constant and low-loss insulating material can reduce the fringe electrical fields into the surrounding media and recover the Q [10]. Therefore, both implanted coils were coated with 1-2 mm biocompatible silicone to measure same Q in saline as in air.

The Q characterization setup is shown in Fig. 5. Coils under test were connected to capacitors forming resonating circuits. By measuring the impedance of the coupled detector coil, the Q factor of the resonating tank (or the coil) under test could be calculated as in the Appendix.

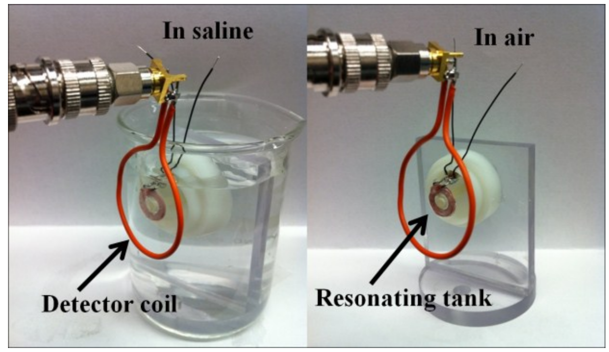

Figure 5. Resonating tank characterization setup in saline. Silicone-coating until the Q recovered to the value in air.

B. System testing in saline

A polycarbonate measurement jig was built, as shown in Fig. 6. The plastic eyeball model can hold the buffer coil and receiver coil in place. The tank is filled with saline to mimic the eye fluid. The protractor on the bottom allows for accurate adjustment of the eye rotation to investigate the efficiency change.

In this prototype, the measured DC voltage across the equivalent DC load is 1.9 V and power consumption is 25.8 mW accordingly. Efficiency of 36.5% with 1 inch separation was measured matching the theoretical calculation (35.9%) and LTspice simulation (35.7%).

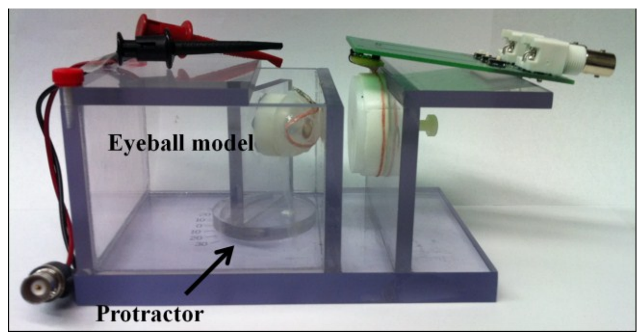

Figure 6. System efficiency measurement jig made of polycarbonate.

C. The efficiency relative to eye rotation

In the 3-coil inductive link, the buffer coil and receiver coil rotate together, which makes the coupling between these coils constant. However there is relative rotation between this coil pair and the transmitter coil. To investigate into the effect of the eyeball rotation on the power transfer efficiency, the stand housing the eyeball model was swept from -30^o to $+30^o$, which corresponds to the viewing angles of eyeball under normal activity [11]. The overall power efficiency change with eyeball rotation angle is shown in Fig. 7. The efficiency can still maintain 14.7% with left and right deflection of 30 degree.

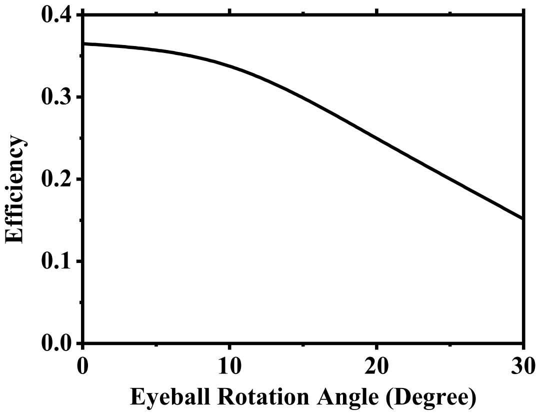

Figure 7. The efficiency change with the eyeball rotation

IV. Conclusion

3-coil wireless power system has demonstrated the feasibility of high power transfer efficiency. The successful fabrication and characterization of the wireless power path facilitate the complete integration of the entire 512-electrode epiretinal prosthesis in the near future. The design and optimization methodology can also be applied to next-generation 1024-electrode retinal prostheses.

Appendix

The detector coil is coupled to the secondary resonating tank. The impedance looking into the detector coil can be measured by the impedance analyzer. The following shows the equivalent circuit schematic and formulas to calculate the quality factor of the coils or resonating tanks.

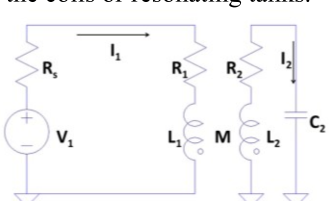

$$\text{Primary loop} \quad : V = Z_1 I_1 + i\omega M I_2$$

$$\text{Secondary loop} \quad : 0 = i\omega M I_1 + Z_2 I_2$$

$$V_1 = Z_1 I_1 + i\omega M\left(-\frac{i\omega M I_1}{Z_2}\right) = Z_1 I_1 + \frac{\omega^2 M^2 I_1}{Z_2} = \left(Z_1 + \frac{\omega^2 M^2}{Z_2}\right) I_1$$

$$\text{Total Impedance} \quad : Z = \frac{V}{I_1} = Z_1 + \frac{\omega^2 M^2}{Z_2}$$

$$Z_2 = R_2 + i\omega L2 + \frac{1}{i\omega C_2}$$

$$\text{When} \quad \omega = \omega_0 + \Delta\omega$$

$$Z_2 = R_2 + i\omega_0 L_2 + i\Delta\omega L_2 + \frac{1}{i\omega_0 C_2 + i\Delta\omega C_2}$$

$$\text{Given} \quad Q_2 = \frac{\omega_0 L_2}{R_2}, \quad \omega_0^2 L_2 C_2 = 1$$

$$\text{When} \quad \Delta\omega = \pm\frac{\omega_0}{2Q}$$

$$Z_2\Big|_{\omega=\omega_0\pm\frac{\omega_0}{2Q}} = R_2 + i\omega_0 L_2 \pm i\frac{\omega_0 L_2}{2Q_2} + \frac{1}{i\omega_0 C_2 \pm i\frac{\omega_0 C_2}{2Q_2}}$$

$$\text{Given} \quad \frac{1}{1+x} = 1 - x, \quad \text{when} \quad x \ll 1$$

$$Z_2\Big|_{\omega=\omega_0\pm\frac{\omega_0}{2Q}} = R_2 + i\omega_0 L_2 \pm i\frac{\omega_0 L_2}{2Q_2} - \frac{i}{\omega_0 C_2}\left(1 \mp \frac{1}{2Q_2}\right)$$

$$\text{Substitute} \quad \frac{\omega_0 L_2}{Q_2} = R_2 \quad \omega_0 C_2 Q_2 = \omega_0 C_2 \frac{\omega_0 L_2}{R_2} = \frac{1}{R_2}$$

$$Z_2\Big|_{\omega=\omega_0\pm\frac{\omega_0}{2Q}} = R_2 \pm i\frac{R_2}{2} \pm i\frac{R_2}{2} = R_2(1 \pm i)$$

$$\text{Because} \quad \frac{\omega_0}{2Q} \ll \omega_0, \quad \omega^2\Big|_{\omega=\omega_0\pm\frac{\omega_0}{2Q}} = \omega_0^2$$

$$Z - Z_1\Big|_{\omega=\omega_0\pm\frac{\omega_0}{2Q}} = \frac{\omega_0^2 M^2}{R_2}\frac{1}{1 \pm i} = \frac{\omega_0^2 M^2}{2R_2}(1 \mp i)$$

The measurement procedure:

- Measure Z_1 without resonant tank coupled
- Read the frequency (f_0) and impedance (Z) corresponding to the peak value with secondary tank coupled
- Read the lower (f_l) and higher (f_h) frequencies where $\mathrm{Re}(Z - Z_1\big|_{\omega=\omega_0\pm\frac{\omega_0}{2Q}}) = \frac{1}{2}\mathrm{Re}(Z - Z_1\big|_{\omega=\omega_0})$
- Q can be calculated as $f_0/(f_h - f_l)$

Acknowledgment

This work is supported by the Biomimetic MicroElectronic Systems (BMES) Center under the grant number H31068. The authors would like to thank Trevor Roper's help in terms of sample preparation, machine maintenance, and instrument installation as well as the members of Caltech Micromachining Laboratory.

References

[1] Weiland, J. D., W. Liu, et al. (2005). "Retinal Prosthesis." Annual Review of Biomedical Engineering 7(1): 361-401.

[2] Ng, D. C., C. E. Williams, et al. (2011). Wireless power delivery for retinal prostheses. Engineering in Medicine and Biology Society,EMBC, 2011 Annual International Conference of the IEEE.

[3] Second Sight, Argus II Retinal Prostheses, http://2-sight.eu/

[4] Lotfi B, M. (2011). Chapter 1 - Building the bionic eye: an emerging reality and opportunity. Progress in Brain Research. C. E. C. J. F. K. Andrea Green and L. Franco, Elsevier. Volume 192: 3-15.

[5] Mokwa, W. (2011). Retinal implants to restore vision in blind people. Solid-State Sensors, Actuators and Microsystems Conference (TRANSDUCERS), 2011 16th International.

[6] Humayun, M, et al. (2007). Book, "Artificial Sight Basic Research, Biomedical Engineering, and Clinical Advances".

[7] RamRakhyani, A. K., S. Mirabbasi, et al. (2011). "Design and Optimization of Resonance-Based Efficient Wireless Power Delivery Systems for Biomedical Implants." Biomedical Circuits and Systems, IEEE Transactions on 5(1): 48-63.

[8] Kiani, M., J. Uei-Ming, et al. (2011). "Design and Optimization of a 3-Coil Inductive Link for Efficient Wireless Power Transmission." Biomedical Circuits and Systems, IEEE Transactions on 5(6): 579-591.

[9] Zhao, Y., M. S. Nandra, et al. (2011). A MEMS intraocular origami coil. Solid-State Sensors, Actuators and Microsystems Conference (TRANSDUCERS), 2011 16th International.

[10] Lin, C. (2012). Thesis, MEMS for Glaucoma

[11] Kelly, S. K., P. Doyle, et al. (2010). Optimal primary coil size for wireless power telemetry to medical implants. Applied Sciences in Biomedical and Communication Technologies (ISABEL), 2010 3rd International Symposium on.